Japanese Journal of Applied Physics
Vol. 46, No. 4A, 2007, pp. 1521–1525

Increased Organic Light-Emitting Diode Panel Light Efficiency by Optimizing Structure and Improving Alignment of Pyramidal Array Light-Enhancing Layers

Ming-Lung CHEN, An-Chi WEI[1]*, and Han-Ping D. SHIEH

Department of Photonics and Display Institute, National Chiao Tung University, Hsinchu, Taiwan 300, R.O.C.
[1]*Department of Photonics and Institute of Electro-Optical Engineering, National Chiao Tung University, Hsinchu, Taiwan 300, R.O.C.*

(Received September 29, 2006; accepted December 22, 2006; published online April 5, 2007)

A pyramidal array light-enhancing layer (pyramidal ALEL) on an organic light-emitting diode (OLED) panel has been optimized to enhance the luminance efficiency with a gain factor of 2.03 experimentally. The issues resulting from the misalignment of the ALEL and OLED pixels were investigated with respect to the effects of the pixel spacing and Moiré pattern. The pixel spacing effect has been shown to be the main cause of gain loss during alignment, whereas the Moiré pattern effect has been shown to be suppressed under the conditions of an appropriate rotational alignment and identical sizes for the ALEL and OLED pixels. [DOI: 10.1143/JJAP.46.1521]

KEYWORDS: organic light-emitting diode (OLED), array light-enhancing layer, light efficiency, alignment, Moiré pattern

1. Introduction

An organic light-emitting diode (OLED) is a potential planar light source and panel display, due to its advantages, such as the high contrast, the sufficient color gamut, the short response time, the wide viewing angle, the small thickness (backlight free) and the light weight. However, only about 20–30% of the emitting light can emerge out of the device.[1)] Methods using rough or textured surfaces, mesa structures, and lenses were employed to overcome efficiency limitations by suppressing waveguide modes.[2–5)] When these structures were applied to an OLED panel, most of incident angles of rays became smaller than the critical angle, and then the total internal reflection (TIR) effect decreased; consequently, the luminance efficiency was improved.

The methods of improving the out-coupling light efficiency of LEDs have also been applied to OLEDs. For example, from the late 1990s, two-dimensional photonic crystals, millimeter-scale silica spheres, corrugated substrates, a silica aerogel layer with a low refractive index, and a method of controlling the thickness of the ITO layer have been exploited to increase the out-coupling light efficiency of LEDs and can be used in OLEDs.[6–11)]

Although many researchers have studied the out-coupling light efficiency of a single OLED pixel, few works on the systematical analysis of array pixels were performed, which is essential for a panel display design. Our pervious study of a multizone light-enhancing layer was demonstrated; however, profile parameters require further optimization and alignment issues, such as the Moiré effect, have not been investigated yet.[12)] Since a pyramidal array light-enhancing layer (ALEL) can be fabricated by standard semiconductor processes, the objective herein is to study the design rules and alignment issues of the pyramidal ALEL on an OLED panel for practical applications.

2. Design

2.1 Optical model

The proposed optical model is described as follows. Light emitting from the active layer of an OLED panel is assumed to go through the pixel array, as shown in Fig. 1. Since organic layers, including the active layer, are much thinner

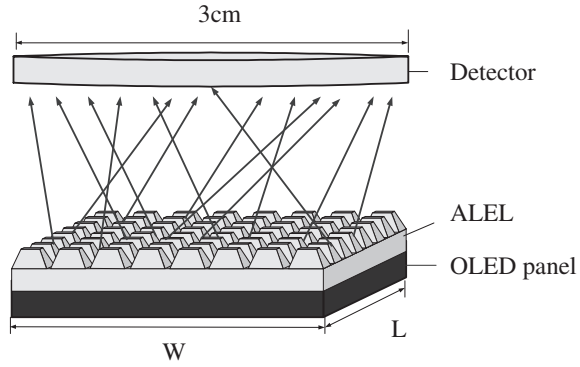

Fig. 1. Optical model of pyramidal ALEL on OLED panel.

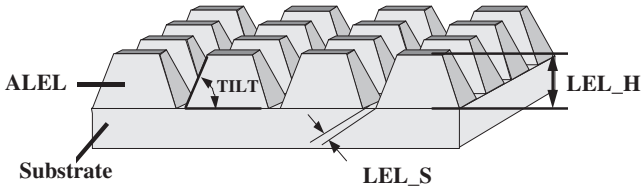

Fig. 2. Illustration of parameters for designing ALEL.

(∼0.15 μm) than the other layers, these organic layers are assumed to be one "source layer" in the simulation.

A flat 3-cm-diameter detector was set to be 3.5 cm above the OLED panel to measure the output flux. The gain factor is defined as the relationship between the flux detected from an OLED panel with the pyramidal ALEL and that detected from a conventional panel:

$$\text{Gain} = \frac{\text{Detected flux of OLED panel with ALEL}}{\text{Detected flux of OLED panel without ALEL}}. \quad (1)$$

As illustrated in Fig. 2, the main parameters of the ALEL structure are the height and tilt angle of each pyramid, and the spacing between adjacent pixels, labeled as LEL_H, TILT, and LEL_S, respectively. The pixel size of the ALEL is designed to fit each pixel of the OLED panel.

2.2 Modeling results

The ray-tracing tool ASAP™ 7.5, which considered also Fresnel equations, was used to examine the optical perform-

*E-mail address: angelwei.eo90g@nctu.edu.tw

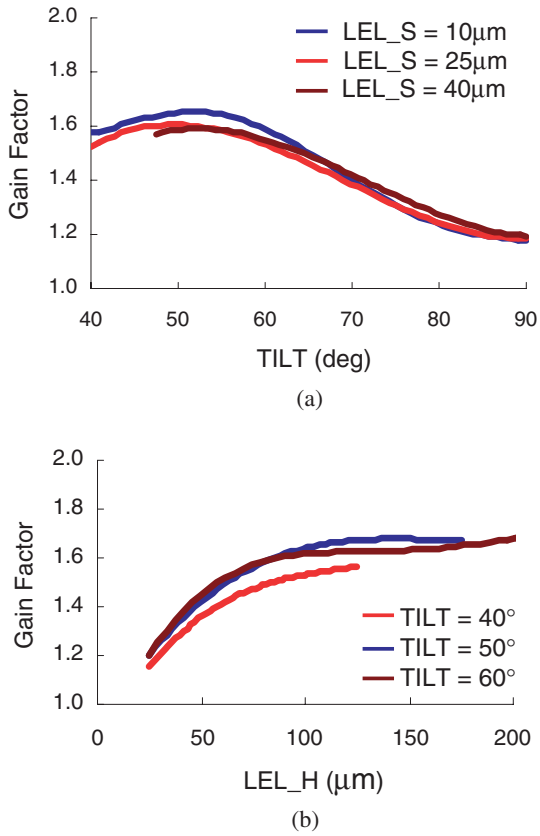

Fig. 3. Simulated gain factor with (a) TILT and LEL_S at LEL_H = 125 μm, and (b) LEL_H and TILT at LEL_S = 10 μm.

ance of the device. The radiation of the light source was assumed to be Lambertian distribution. The material of the ALEL was assumed to be poly(dimethylsiloxane) (PDMS) with the refractive index of 1.46, whereas the height of the ALEL was controlled within 200 μm. The target OLED panel was a device with 70 × 70 pixels. On the basis of the simulated results shown in Fig. 3(a), the maximal gain can be obtained with structures with the tilt angle range of 50 to 55°. Meanwhile, when the tilt angle ranges from 50 to 60°, a small spacing can lead to a high gain. Moreover, the gain reaches the maximum when the height is larger than 100 μm, as shown in Fig. 3(b). In a chromatic analysis, the emission wavelengths of 780, 550, and 318 nm resulted in the same gain factor, indicating that the wavelengths in the visible spectrum do not affect the performance of the designed ALEL.

3. Fabrication

The fabrication of the ALEL comprises standard semiconductor fabrication processes and plastic molding replication techniques. The semiconductor fabrication processes can be categorized as the bulk micromachining technique in the micro-electro-mechanical system (MEMS). First, a mask layer of 0.5-μm-thick SiN_x was deposited on a silicon wafer with a (100) surface orientation by plasma-enhanced chemical vapor deposition (PECVD). Next, photolithography was applied to define the pixel size of the ALEL with the photoresist (PR) AZ4620, G-line exposure and developer AZ300. Subsequently, reactive ion etching (RIE) was performed to transfer the pattern from the PR to the mask layer. Then, acetone cleaning and KOH wet etching were performed to remove the residual PR and to form the desired structure on the silicon mold, respectively. To fabricate the ALEL, the mold was pretreated with an antisticking layer (1*H*,1*H*,2*H*,2*H*-perfluorodecyl trichlorosilane) to prevent PDMS from adhering to the mold during replication. Subsequently, the mold was filled with PDMS. After removing bubbles using a vacuum chamber and curing at 50 °C for 3 h, we peeled off the flexible PDMS from the mold and completed the fabrication of the ALEL, as illustrated in Fig. 4.

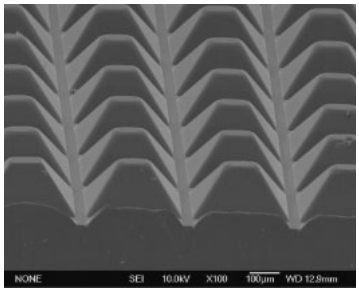

Fig. 4. SEM image of ALEL.

4. Measurement and Discussion

The optical performance, evaluated using the luminance in a direction normal to the OLED panel, was measured using a Minolta CS-100 chromameter and a ConoScope™ in a dark room.

4.1 Optimization of ALEL parameters

Since the simulated results indicated that TILT ranging from 50 to 55° could lead to the maximal gain and that conventional silicon bulk micromachining could realize a structure with a tilt angle of 54.7°, TILT was fixed at 54.7° for the following experiments. To examine the optimization of the other two parameters, LEL_H and LEL_S, the ALEL samples were fabricated with different heights and spacings. At the optimum alignment, the measured results shown in Fig. 5 reveal that the maximal gain can be derived from a sufficient height and a smaller spacing, agreeing with the simulated results. The maximum gain factor of 2.03 was measured using the optimized structure of LEL_S = 15 μm and LEL_H = 200 μm. Meanwhile, before and after the

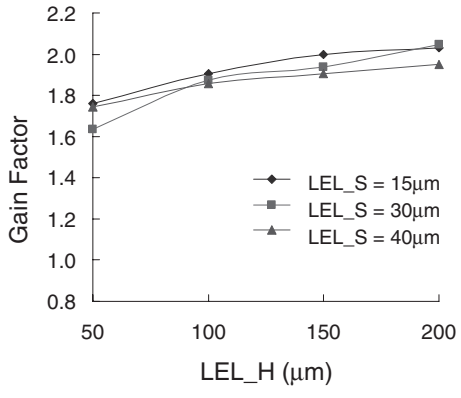

Fig. 5. Relationship between gain factor and LEL_H at TILT = 55°.

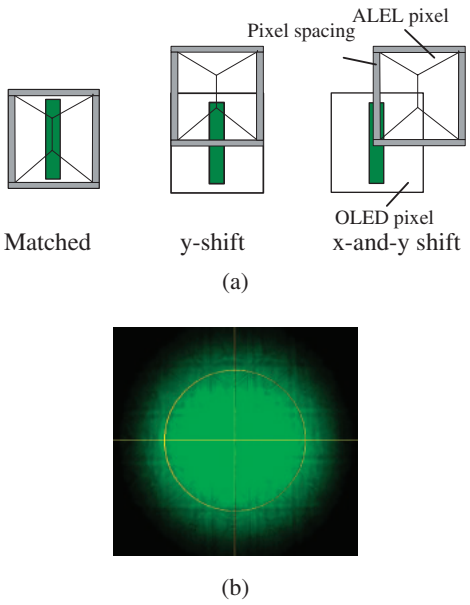

Fig. 6. Gain factor losses of three ALEL alignment cases: matched, *y*-shift and *x*-and-*y* shift; (a) schematics of top view and (b) image of alignment mark aimed at center of ALEL pixel.

attachment of the ALEL, the measured difference in color gamut was $(\Delta x, \Delta y) = (0.003, 0.003)$ in a CIE 1931 chromaticity diagram, exhibiting a nonsignificant variance and thus agreeing with the result of our chromatic analysis.

4.2 *Alignment*

Once the structure of the pyramidal ALEL was optimized, the next considerations were the practical implementation of the ALEL on an OLED panel. In particular, the alignment of the ALEL and OLED pixels should be well controlled. To analyze these alignment issues, the phenomena are investigated from two perspectives: the effect caused by the pixel spacing of the ALEL and the cause of the Moiré pattern.

4.2.1 *Pixel spacing of ALEL*

The pixel spacing of the ALEL is defined as the flat border of each ALEL pixel, as shown in Fig. 6. The issue resulting from the alignment of the pixel spacing is then investigated. Consider a misalignment between the ALEL and OLED pixels along the *y*-direction (*y*-shift). The *x*-orientation spacing of the ALEL crosses the *y*-orientation light source and reduces the gain factor, as illustrated in the middle drawing in Fig. 6(a). However, the gain loss in the alignment is dominated by the *x*-directional misalignment (*x*-shift) due to a large cross area. Thus, it can be expected that such misalignments with an *x*-shift will cause a severer loss than the only *y*-shift case, as shown in the right-hand-side drawing in Fig. 6(a). Such a gain loss resulting from the *x*- or *y*-directional shift is called the pixel spacing effect in this study.

Experimental inspection was first performed by aiming the alignment mark at the center of an ALEL pixel without lighting the source, as shown in Fig. 6(b). When switching on the light source, we detected three types of alignment: matched, *y*-shift, and *x*-and-*y* shift, whereas the measured gain factors were 1.95, 1.62, and 0.93, respectively. Such results show that the case of the *x*-and-*y* shift has the largest overlapping area and the highest gain loss, which consists with the speculation of the pixel spacing effect. Therefore, the small spacing of the ALEL pixels, resulting in a small overlapping area, is expected to inhibit the pixel spacing effect and thus to contribute to the gain.

4.2.2 *Moiré pattern*

To investigate another Moiré pattern issue, several alignment cases are illustrated in Fig. 7 for comparison. An OLED panel with the matched ALEL pixels is the desired case that is free from Moiré patterns, as shown in case 1. Also, it can be observed that although the *x*- or *y*-shift exists, no Moiré pattern is formed. On the other hand, due to the interference resulting from the mismatched edge periods of the ALEL and OLED pixels, Moiré patterns are more obvious in cases 2 and 3, which have rotational misalignment and *x*–*y* reverse, respectively. In addition, the rotated ALEL pixels in case 2 cause the corner overlap of the ALEL and OLED pixels, which results in the pixel spacing effect

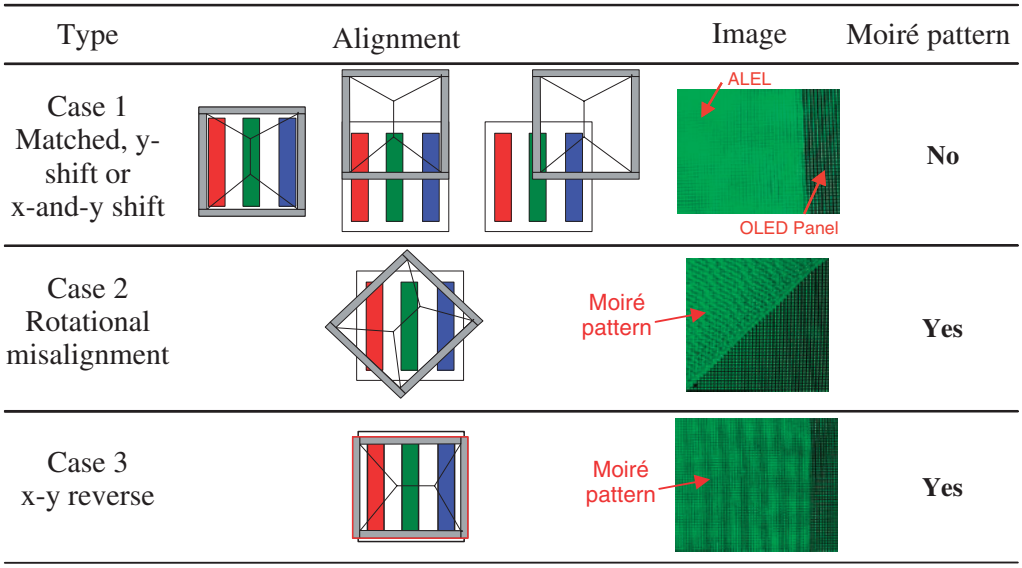

Fig. 7. Moiré patterns of various alignment cases.

and reduces the gain factor. In case 3, owing to the different periods along the x- and y-axes, the case with x–y reverse also causes the overlap of the ALEL spacing and OLED light source, again resulting in the pixel spacing effect.

Such a phenomenon can be elucidated using the well-known Moiré formula. When the ALEL is rotated at an angle of θ with respect to the x-axis, the Moiré periods resulting from the periods of the ALEL along the x- and y-axes, W_x and W_y, can be derived as

$$W_x = \frac{P_{Ax}P_0}{\sqrt{P_{Ax}^2 + P_0^2 - 2P_{Ax}P_0\cos\theta}}, \quad (2)$$

and

$$W_y = \frac{P_{Ay}P_0}{\sqrt{P_{Ay}^2 + P_0^2 - 2P_{Ay}P_0\sin\theta}}, \quad (3)$$

where P_{Ax} and P_{Ay} are the periods of the ALEL along the x- and y-axes, respectively. Since the orientation of the OLED pixels is along the y-axis, the x-period of the OLED pixels, P_0, is dominated and considered. In addition, because the ALEL pixels are designed to have the same size as the OLED pixels, i.e., $P_{Ax} = P_0$, W_x is

$$W_x = \frac{P_0}{\sqrt{2(1-\cos\theta)}}. \quad (4)$$

Assume that the period of the OLED pixels (P_0) is too small to be perceived by human eyes. If the Moiré periods can be reduced to a level near P_0, the Moiré patterns shall be imperceptible. For the rotational misalignment case, such as case 2, a Moiré pattern can be observed and modeled using eqs. (3) and (4) herein. For extreme cases, such as case 1, θ is zero, resulting in an infinite W_x; thus, no Moiré pattern is formed along the x-direction. Meanwhile, since P_{Ay} and P_0 are in the same order in our experiment, W_y in case 1 is near P_0. As a result, the Moiré pattern along the y-direction is also not observed. As for case 3 with $\theta = \pi/2$, W_x and W_y can be derived as

$$W_x = \frac{P_0}{\sqrt{2}}, \quad (5)$$

and

$$W_y = \frac{P_0P_{Ay}}{P_0 - P_{Ay}}. \quad (6)$$

Although the Moiré period of W_x is beyond perception, the pattern resulting from W_y is still effective. Therefore, case 3 displays obvious Moiré fringes.

The above-mentioned results can be used to obtain the following two points. First, gain factor losses during the alignment are closely related to the pixel spacing effect. To eliminate the pixel spacing effect, a small spacing between ALEL pixels is recommended. Second, when ALEL pixels fit OLED pixels without rotational misalignment, even if there are ALEL shifts along the x- and y-axes, the observers do not perceive Moiré patterns.

4.3 Discussion

For comparison, two prior literatures are referred to.[4,5] According to Wei and Su's results,[5] a significant improvement in luminance efficiency was observed when the width of the microlens and the pixel spacing were set to be 100 and 11 μm, respectively. Another research performed by Möller and Forrest involved the adoption of the microlens array with a pixel diameter of 10 μm.[4] These parameters and experimental results are summarized in Table I. It is shown that our proposed structure has a comparable gain of 2.03.

Table I. Parameters and experimental results for different structures.

Architecture	Pixel diameter (μm)	Pixel spacing (μm)	Height (μm)	Gain factor
Without ALEL	—	—	—	1.00
Microlens 1[5]	100	11	~50	1.50
Microlens 2[4]	10	~0	~5	1.56
Proposed structure	~300	15	150	2.03

The high luminance efficiency of the proposed structure results from the identical sizes design for the ALEL and OLED pixels. As a result, most of the light entering the proposed ALEL can be extracted from the device when it is first incident upon the ALEL-air interface, whereas microlens methods result in more reflections at the microlens-air interface. Although such reflected light can be retrieved by total internal and electrode reflections inside the OLED device, the transmittance of the upper electrode and the reflectance of the bottom electrode are not prefect unity, resulting in that the higher the number of reflections light encounters, the higher the loss it suffers. Therefore, to enhance the luminance efficiency, our identical size design for the ALEL and OLED pixels is preferred.

However, when the alignment tolerance and image quality are considered, the proposed ALEL design might not have a better performance than the microlens methods. Since the diameter of the microlens is typically 10 times smaller than one OLED pixel and the distribution of the microlens is uniform, any orientation or shift leads to a similar contribution; consequently, there is no requirement of alignment for the microlens and OLED. As for the image quality, the microlens methods result in blurring,[4] whereas the proposed ALEL magnifies the OLED pixels and then produces coarse images. To overcome these issues, the advanced instrument can lead to a sufficient alignment accuracy, whereas the finer OLED pixel design can lead to a finer ALEL pixel and the elaborate images.

On the other hand, compared with commercial light control films used in thin film transistor liquid crystal displays (TFT-LCDs), the ALEL with a thickness of around 3 mm (including the heights of the base and pyramid) is thick. To reduce the ALEL thickness, PDMS can be replaced by polyester (PET), whose processing is widely used in optical film manufacturing and can lead to a base with a micrometer-scaled thickness. Moreover, the height of the pyramid can be reduced if such a refractive element is replaced by a diffractive element (DOE) surface. Furthermore, with a random orientation technique, such as the use of a multidirectional asymmetrical microlens array,[13] the DOE-type ALEL can not only have a small thickness but also suppress the formation of Moiré patterns.

5. Conclusions

A light-enhancing layer with a pyramidal array (pyramidal ALEL) on an OLED panel has been successfully

demonstrated. The presented pyramidal ALEL with a tilt angle of 54.7° fabricated by bulk micromachining processes has an optimized gain factor. Both simulated and measured results show that the pyramidal ALEL can enhance the luminance efficiency more conspicuously with a small pixel spacing and a sufficient pyramid height. Experimentally, the device constructed with the optimized pyramidal ALEL can yield a gain factor of 2.03. Moreover, the alignment issues between the ALEL and the OLED have been investigated in terms of the pixel spacing and Moiré pattern effects. The former effect, resulting from the overlap of the spacing between adjacent ALEL pixels and the emitting pixel of the OLED panel, causes gain loss and is the main effect of misalignment. To suppress this effect, decreasing the spacing between adjacent ALEL pixels is recommended. Meanwhile, the Moiré pattern effect can be avoided when ALELs and OLEDs have an identical pixel size and an appropriate rotational alignment, even if the ALEL has shifts along both x- and y-axes. By replacing PDMS with PET and using a DOE surface, the ALEL thickness can be reduced. Therefore, both pixel spacing effect and Moiré pattern issues shall be overcome; as a result, an appropriate alignment and an optimized light efficiency of OLED panels shall be achieved using the pyramidal ALEL.

Acknowledgement

This work was partially supported by Chuanghwa Picture Tubes, Ltd.

1) C. F. Madigan, M.-H. Lu, and J. C. Sturm: Appl. Phys. Lett. **76** (2000) 1650.
2) A. A. Bergh and R. H. Saul: U.S. Patent 3739217 (1973).
3) I. Schnitzer, E. Yablonovitch, C. Caneau, T. J. Gmitter, and A. Scherer: Appl. Phys. Lett. **63** (1993) 2174.
4) S. Möller and S. R. Forrest: J. Appl. Phys. **91** (2002) 3324.
5) M. K. Wei and I. L. Su: Opt. Express **12** (2004) 5777.
6) S. H. Fan, P. R. Villeneuve, J. D. Joannopoulos, and E. F. Schubert: Phys. Rev. Lett. **78** (1997) 3294.
7) M. Boroditsky, R. Vrijen, T. F. Krauss, R. Coccioli, R. Bhat, and E. Yablonovitch: J. Lightwave Technol. **17** (1999) 2096.
8) T. Yamasaki, K. Sumioka, and T. Tsutsui: Appl. Phys. Lett. **76** (2000) 1243.
9) B. J. Matterson, J. M. Lupton, A. F. Safonov, M. G. Salt, W. L. Barnes, and I. D. W. Samuel: Adv. Mater. **13** (2001) 123.
10) T. Tsutsui, M. Yahiro, H. Yokogawa, K. Kawano, and M. Yokoyama: Adv. Mater. **13** (2001) 1149.
11) M. H. Lu and J. C. Sturm: J. Appl. Phys. **91** (2002) 595.
12) A. C. Wei and H. P. D. Shieh: Jpn. J. Appl. Phys. **45** (2006) 4115.
13) Y. P. Huang, J. J. Chen, F. J. Ko, and H. P. D. Shieh: Jpn. J. Appl. Phys. **41** (2002) 646.